European Review for Medical and Pharmacological Sciences 2020; 24: 3526-3537

Silencing of lncRNA XIST suppresses proliferation and autophagy and enhances vincristine sensitivity in retinoblastoma cells by sponging miR-204-5p

L. YAO[1], L. YANG[2], H. SONG[3], T.-G. LIU[4], H. YAN[1]

[1]Department of Ophthalmology, Tianjin Medical University General Hospital, Tianjin, China
[2]Department of Tianjin Key Laboratory, Tianjin Nankai Hospital, Tianjin, China
[3]Department of Ophthalmology, Tianjin Eye Hospital, Tianjin, China
[4]Department of Ophthalmology, Beijing Capital International Airport Hospital, Beijing, China

Abstract. – OBJECTIVE: Retinoblastoma (RB) is the most prevalent intraocular malignancy in childhood. Long non-coding RNAs (lncRNAs) have been found as critical oncogenic drivers and tumor suppressor in RB. The aim of the present work was to investigate the impact and mechanism of XIST on RB cell autophagy and vincristine (VCR) sensitivity.

MATERIALS AND METHODS: The levels of XIST and miR-204-5p were assessed by quantitative Real Time-Polymerase Chain Reaction (qRT-PCR). Western blot analysis was used for the determination of related protein levels. Cell proliferation and IC50 value of VCR were detected using the 3-(4,5-dimethylthiazol-2-yl)-5-(3-carboxymethoxyphenyl)-2-(4-sulfophenyl)-2H-tetrazolium (MTS) assay. Flow cytometry was performed to evaluate cell apoptosis. The activities of caspase-3 and caspase-9 were identified using a corresponding assay kit. The direct interaction between XIST and miR-204-5p was confirmed using Dual-Luciferase reporter assay. Xenograft model was established to observe the effect of XIST on RB *in vivo*.

RESULTS: Our data indicated that XIST was highly expressed in RB tissues and cell lines. XIST knockdown weakened the proliferation and autophagy and enhanced VCR sensitivity in RB cells. XIST acted as a molecular sponge of miR-204-5p. Moreover, the regulatory effects of XIST silencing on RB cell proliferation, autophagy and VCR sensitivity were mediated by miR-204-5p. Additionally, XIST silencing weakened tumor growth and enhanced VCR sensitivity *in vivo* through up-regulating miR-204-5p.

CONCLUSIONS: Our current study suggested that XIST silencing suppressed RB progression and promoted VCR sensitivity *in vitro* and *in vivo* at least partially by acting as a miR-204-5p sponge, highlighting a powerful therapeutic strategy for RB treatment.

Key Words:
RB, XIST, MiR-204-5p, Autophagy, VCR sensitivity.

Introduction

Retinoblastoma (RB) is the most prevalent intraocular malignancy in childhood and affects about one infant in 15,000-20,000 live births around the world[1,2]. Despite the great improvement of therapeutic agents, effective treatments against RB are still limited[3]. Thus, a better understanding of the mechanism involved in the development and progression of RB is pivotal.

Non-coding RNAs (ncRNAs) have been found as critical oncogenic drivers and tumor suppressors in human cancer[4]. The functional relevance of the ncRNAs is particularly evident for a class of long ncRNAs (lncRNAs) and microRNAs (miRNAs)[5,6]. LncRNAs are longer than 200 nucleotides transcripts that have been identified as essential players in RB tumorigenesis[7]. Notably, lncRNAs exert biological function in RB progression through the regulatory network of the competing endogenous RNA (ceRNA) by sponging specific miRNAs[8-10].

X-inactive specific transcript (XIST), a 17 kb lncRNA located on the X chromosome, has been reported to accelerate tumorigenesis and progression in a large number of human cancers, such as colorectal cancer, non-small cell lung, and osteosarcoma[11-13]. Moreover, highly expressed XIST was closely associated with chemoresistance to drugs in tumor cells[14,15]. In RB, XIST was demonstrated to be upregulated in RB tissues and cells,

Corresponding Author: Hua Yan, MD; e-mail: hanzxu@163.com

and its deficiency suppressed RB progression by acting as a ceRNA[16,17]. Herein, we aimed to investigate the impact and mechanism of XIST on RB cell autophagy and vincristine (VCR) sensitivity.

MiR-204-5p level was significantly reduced in RB, and enforced expression of miR-204-5p hampered RB cell progression *via* the regulation of cell viability, invasion, and apoptosis[18,19]. A potential target site of XIST and miR-204-5p was predicted using starBase v.3 software, hinting a regulatory network of the XIST/miR-204-3p axis. In the present work, our data supported a significant upregulation of XIST in RB tissues and cells. Consequently, the influence and mechanism of XIST on RB cell proliferation, autophagy, and VCR sensitivity were observed *in vitro* and *in vivo*.

Materials and Methods

Clinical Samples

In the current study, 31 fresh tissue samples, including 25 RB tissues and 6 matched normal retinal tissues, were collected following enucleation from Tianjin Medical University General Hospital. These patients with RB were all under the age of five years, and the informed consent was signed by their parents or legal guardians before surgery. These samples were stored at -80°C until use. The protocol for the use of clinical samples was approved by the Ethics Committee of Tianjin Medical University General Hospital.

Cell Culture, Treatment and Transfection

Two RB cell lines WERI-RB1 (ATCC®HTB-169) and Y79 (ATCC®HTB-18) and human pigment retinal epithelial ARPE-19 cell line (ATCC®CRL-2302) were obtained from the American Type Culture Collection (ATCC; Manassas, VA, USA). ARPE-19 cells were maintained in Dulbecco's Modified Eagle's Medium/Nutrient Mixture F-12 (DMEM/F-12; Gibco, Rockville, MD, USA) and RB cells were grown in Roswell Park Memorial Institute-1640 (RPMI-1640) medium (Gibco, Rockville, MD, USA) plus 10% fetal calf serum (FCS; Bovogen Biologicals, Keilor East VIC, Australia) at 37°C in a 5% CO_2 atmosphere. For VCR treatment, WERI-RB1 and Y79 cells were exposed to various concentrations (0, 0.015625, 0.03125, 0.0625, 0.125, 0.25, 0.5 and 1 μg/mL) or 0.1 μg/mL of VCR (Sigma-Aldrich, St. Louis, MO, USA) for 48 h for the determination of IC_{50} and cell apoptosis.

The sequences of XIST were cloned into the pcDNA3.1 plasmid (Promega, Madison, WI, USA) using the genetic engineering method[20] to construct XIST overexpression vector (pcDNA-XIST), and nontarget plasmid (pcDNA-NC) was used as the negative control. When the confluence of WERI-RB1 and Y79 cells reached 40-60%, 20 ng of pcDNA-XIST or pcDNA-NC, 50 nM of siRNA against XIST (si-XIST, GenePharma, Shanghai, China) or siRNA negative control (si-NC, GenePharma, Shanghai, China), 50 nM of miR-204-5p mimic (GenePharma, Shanghai, China) or mimic negative control (miR-NC mimic, GenePharma, Shanghai, China), 50 nM of miR-204-5p inhibitor (anti-miR-204-5p, GenePharma, Shanghai, China) or inhibitor negative control (anti-miR-NC, GenePharma, Shanghai, China) were transfected into cells using the Lipofectamine 3000 reagent (Thermo Fisher Scientific, Waltham, MA, USA). The primers sequences were listed as follows: si-XIST: 5'-GCUGACUACCUGAGAUUUATT-3', si-NC: 5'-UUCUCCGAACGUGUCACGU-3', miR-204-5p mimic: 5'-UUCCCUUUGUCAUCCUAUGCCU-3', miR-NC mimic: 5'-CAUUGCACUUGUCUCGGUCUGA-3', anti-miR-204-5p: 5'-AGGCAUAGGAUGCAAAGGGAA-3', anti-miR-NC: 5'-UCUACUCUUUCUAGGAGGUUGUGA-3'.

Quantitative Real Time-Polymerase Chain Reaction (qRT-PCR)

The TRIzol reagent (Thermo Fisher Scientific, Waltham, MA, USA) was used for RNA isolation from RB tissues and cells, referring to the protocols of manufacturers. A total of 1 μg of RNA extracts was used to synthesize cDNA by using Reverse Transcription Master Mix (TaKaRa, Dalian, China) with random primers or TaqMan MicroRNA Reverse Transcription Kit (Applied Biosystems, Foster City, CA, USA) with miRNA-specific primers. Synthesized cDNA was then subjected to qRT-PCR using SYBR Green PCR Master Mix (Applied Biosystems, Foster City, CA, USA) on the 7500 Real-Time System (Applied Biosystems, Foster City, CA, USA). Relative expression levels of XIST and miR-204-5p were calculated by the $2^{-\Delta\Delta Ct}$ method with glyceraldehyde-3-phosphate dehydrogenase (GAPDH) or U6 as the endogenous control. Primers sequences used in this study were listed as follows: XIST: 5'-TCAGCCCATCAGTCCAAGATC-3' (forward) and 5'-CCTAGTTCAGGCCTGCTTTTCAT-3' (reverse); GAPDH: 5'-AAGGTGAAGGTCGGAGTCAAC-3' (forward) and 5'-GGGGTCATTGATGGCAACAATA-3' (re-

verse); miR-204-5p: 5'-AACCTGATCCCGTCTGAGATTG-3' (forward) and 5'-CCGGATCAAGATTAGTTCGGTT-3' (reverse); U6: 5'-CTCGCTTCGGCAGCACA-3' (forward) and 5'-AACGCTTCACGAATTTGCGT-3' (reverse).

Subcellular Fractionation

A commercial Cytoplasmic & Nuclear RNA Purification Kit (Norgen Biotek, Thorold, ON, Canada) was used to extract RNA from cytoplasmic and nuclear fractions. The level of XIST was assessed by qRT-PCR, with GAPDH and U6 as the internal control.

Western Blot

The preparation of total protein from RB tissues and cells was performed as previously described[21]. A total protein of 50 μg was resolved on the 10% sodium dodecyl sulphate (SDS) polyacrylamide gel electrophoresis (PAGE) and electrophoretically blotted onto the polyvinylidene difluoride (PVDF) membranes (Hybond P, GE Healthcare, Diegem, Belgium). The blots were incubated with primary antibodies overnight at 4°C and then incubated with horseradish peroxidase (HRP)-conjugated goat anti-rabbit or anti-mouse IgG (Abcam, Cambridge, UK) as the secondary antibodies. The immunoreaction was detected using the West Femto Maximum Sensitivity Substrate (Pierce, Rockford, IL, USA). The following primary antibodies were obtained from Abcam: anti-p62 (1:1,000), anti-Ki-67 (1:500), anti-proliferating cell nuclear antigen (anti-PCNA, 1:5,000), anti-B cell lymphoma 2 (anti-Bcl-2, 1:1,000), anti-Bax (anti-Bax, 1:5,000) and anti-GAPDH (1:10,000). The primary antibodies were obtained from Cell Signaling Technology (CST; Danvers, MA, USA): anti-light chain 3B-I (anti-LC3B-I, 1:1,000) and anti-LC3B-II (1:1,000).

Measurement of Cell Proliferation and IC50 Value

Assessment of cell proliferation and IC50 value of VCR was carried out using the 3-(4,5-dimethylthiazol-2-yl)-5-(3-carboxymethoxyphenyl)-2-(4-sulfophenyl)-2H-tetr-azolium (MTS) colorimetric assay. In cell proliferation assay, WERI-RB1 and Y79 cells grown in 96-well plates were transfected with si-NC, si-XIST, si-XIST+anti-miR-NC or si-XIST+anti-miR-204-5p for 0, 24, 48 and 72 h. In the determination of IC50 value, transfected cells were exposed to various concentrations (0, 0.015625, 0.03125, 0.0625, 0.125, 0.25, 0.5 and 1 μg/mL) of VCR for 48 h. In both assays, 10 μL of MTS solution was used followed by the incubation at 37°C for 2-4 h, referring to the instructions of the CellTiter 96® Aqueous One solution Cell Proliferation Assay Kit (Promega, Madison, WI, USA). Viability was defined as the absorbance of formazan at OD490 nm by using a ChroMate 4300 microplate reader (Awareness Technologies Inc., Westport, CT, USA).

Determination of Cell Apoptosis

Apoptosis of WERI-RB1 and Y79 cells after transfection and VCR treatment was evaluated using flow cytometry. Treated cells were double-stained with 10 μL of Annexin V-FITC and 5 μL of propidium iodide (PI; Thermo Fisher Scientific, Waltham, MA, USA) for 15 min in the dark. Lastly, the apoptotic rate was analyzed using a FACScan flow cytometer (BD Biosciences, Franklin Lakes, NJ, USA).

Activity Detection of Caspase-3 and Caspase-9

The activities of caspase-3 and caspase-9 were evaluated using the commercial Caspase-3 Activity Assay Kit and Caspase-9 Activity Assay Kit (all from Beyotime, Shanghai, China), following the producer's guidance. The activities were proportional to the absorbance which could be measured using the microplate reader at OD405 nm.

Bioinformatics and Dual-Luciferase Reporter Assay

The directly interacted miRNAs of XIST were predicted using starBase v.3 software at http://starbase.sysu.edu.cn/. XIST wild-type Luciferase reporter plasmid (XIST-WT) containing the miR-204-5p-binding sequence and its mutant of the seed region (XIST-MUT) were synthesized by HanBio (Shanghai, China). 20 ng of XIST-WT or XIST-MUT was transfected into WERI-RB1 and Y79 cells together with miR-NC mimic or miR-204-5p mimic. *Renilla* and firefly Luciferase activities were synchronously detected 48 h post-transfection using the Dual-Luciferase Reporter Assay System (Promega, Madison, WI, USA).

Lentiviral Vector Transduction

Lentiviral particles harboring shRNA targeting XIST (sh-XIST) or nontarget oligonucleotide sequence (sh-NC) were constructed by Fulengen (Guangzhou, China). Y79 cells were infected by lentiviruses-encoding sh-NC or sh-XIST with

various multiplicities of infection in RPMI-1640 medium containing 8 μg/mL of polybrene. 24 h later, cells with positive transduction were selected by puromycin (Tocris Bioscience, Bristol, UK) at a final concentration of 10 μg/mL.

In Vivo Assay

Male BALB/c nude mice (5-7 weeks, n = 24) were bought from Henan Research Center of Laboratory Animal (Zhengzhou, China). These mice were equally divided into four groups (n = 6): sh-NC, sh-XIST, sh-NC+VCR, or sh-XIST+VCR. Approximately 1.0×10^7 Y79 cells stably transduced sh-NC or sh-XIST were subcutaneously inoculated into the nude mice. 7 days after injection, VCR (1 mg/kg) or phosphate-buffered saline (PBS) was injected intraperitoneally every 3 days. Tumor volume was measured with calipers every 3 days after 7 days implantation. At the end of the experiments, all mice were euthanized, and tumor tissues were excised for weight and qRT-PCR. All animal procedures were conducted according to the National Standard for the Care and Use of Laboratory Animals and the protocol of the animal study was approved by the Animal Ethics Committee of Tianjin Medical University General Hospital.

Statistical Analysis

Differences of two groups were determined by a Student's *t*-test, and multiple sets of data were compared by one-way analysis of variance (ANOVA) followed by post-hoc Dunnett's tests using GraphPad Prism (GraphPad Software, La Jolla, CA, USA). Spearman test was used to identify the correlation between XIST expression and miR-204-5p level in RB tissues. Statistical significance is denoted by $*p<0.05$.

Results

Upregulation of XIST In RB Tissues and Cell Lines

First, we evaluated the expression pattern of XIST in RB tissues and cells using qRT-PCR. These results showed that XIST expression was significantly increased in RB tissues compared with the matched normal retinal tissues (Figure 1A). Consistently, XIST level was higher in RB cells than that of normal control (Figure 1B). We then analyzed the subcellular localization of XIST in WERI-RB1 and Y79 cells. As demonstrated in Figure 1C and 1D, XIST was prominently present in the cytoplasm fraction (Figure 1C and 1D). Of note, Western blot

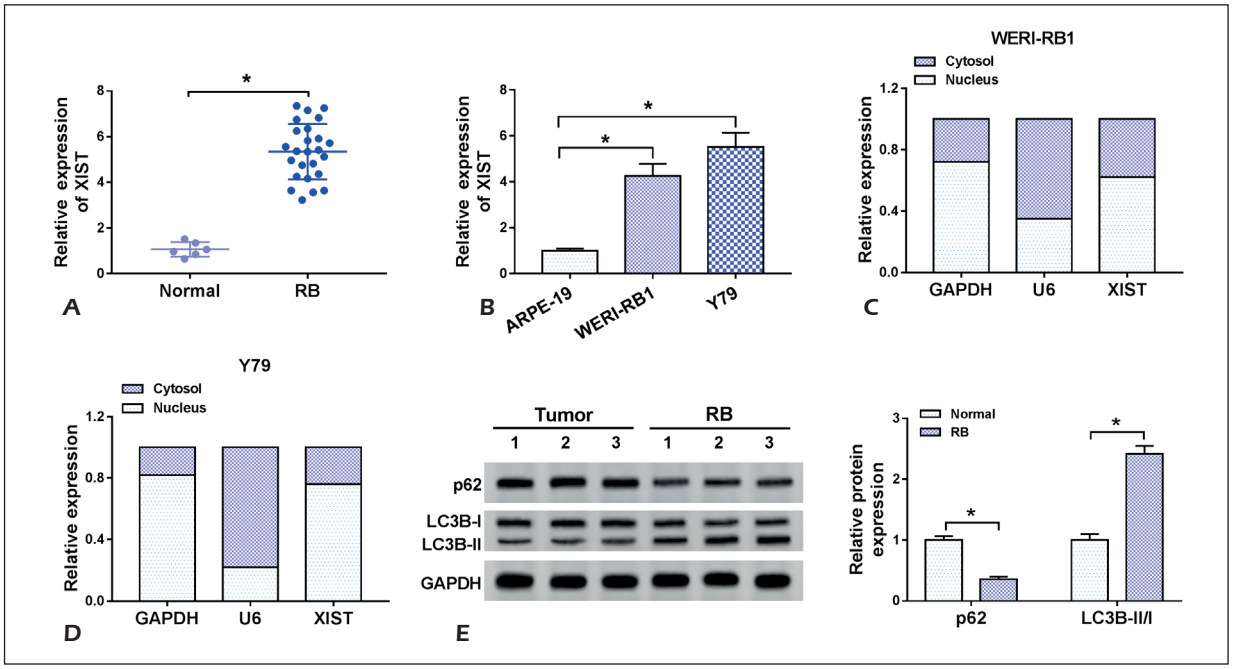

Figure 1. XIST expression was increased in RB tissues and cells. XIST expression by qRT-PCR in RB tissues and the matched normal retinal tissues (**A**), ARPE-19, WERI-RB1, and Y79 cells (**B**). **C-D**, The subcellular localization of XIST in the nuclear and cytoplasm fractions of WERI-RB1 and Y79 cells. **E**, The expression levels of LC3B-II, LC3B-I, and p62 by Western blot in RB tissues and the matched normal retinal tissues. $*p<0.05$.

data revealed that in contrast to normal controls, a higher LC3B-II/I ratio and a lower p62 level were found in RB tissues (Figure 1E), implying the involvement of autophagy in RB progression.

Silencing of XIST Weakened the Proliferation and Autophagy In RB Cells

To explore the role of XIST in RB progression, we performed "phenocopy" silencing by siRNA against XIST. Transient transfection of si-XIST, but not a scrambled negative sequence, prominently decreased the expression of XIST in both WERI-RB1 (67% reduction) and Y79 (58% reduction) cells (Figure 2A). MTS results revealed that compared with the negative group, XIST knockdown triggered a significant inhibition in cell proliferation (Figure 2B and 2C). Moreover, the data of Western blot analysis showed that XIST depletion resulted in decreased expression of proliferating markers Ki-67 and PCNA in the two RB cells (Figure 2D and 2E), supporting the repression of XIST silencing on cell proliferation. Additionally, a lower LC3B-II/I ratio and a higher p62 level were validated in the two XIST-silencing RB cells (Figure 2F and 2G), suggesting the suppressive effect of XIST knockdown on cell autophagy.

Silencing of XIST Enhanced RB Cell Sensitivity to VCR

Then, we observed whether XIST depletion influenced VCR resistance of RB cells. In comparison to a corresponding negative control, the analysis of MTS revealed that XIST knockdown resulted in decreased IC_{50} value of VCR in both WERI-RB1 and Y79 cells (Figure 3A-3D). Flow cytometry assays showed that XIST silencing enhanced cell apoptosis in the two RB cells after VCR treatment (Figure 3E and 3F). Moreover, XIST depletion led to an evident repression in Bcl-2 expression and a clear promotion in Bax level, as well as a significant activity enhancement in caspase-3 and caspase-9 (Figure 3G-3J).

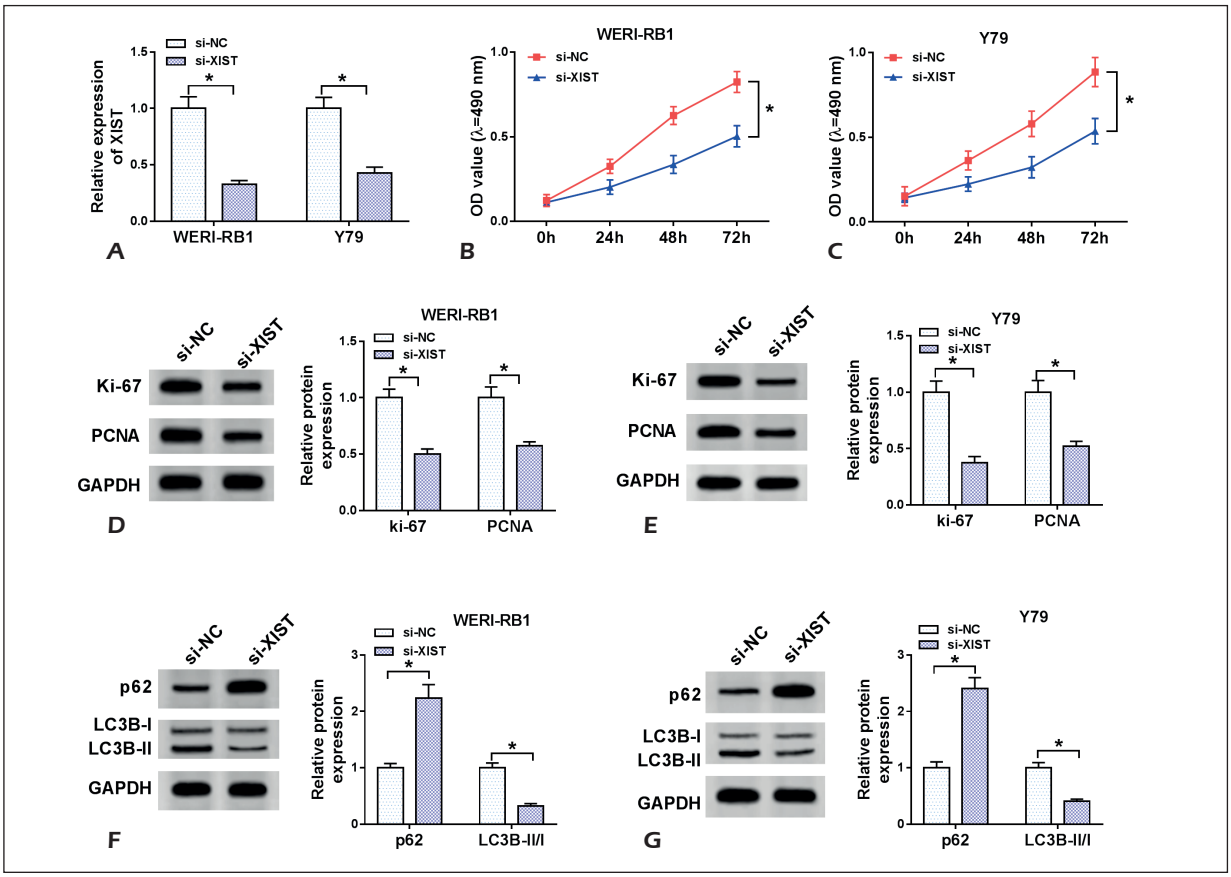

Figure 2. XIST silencing hampered RB cell proliferation and autophagy. WERI-RB1 and Y79 cells were transfected with si-NC or si-XIST for the indicated time. **A**, qRT-PCR for XIST expression after 48 h transfection in transfected cells. **B**, and **C**, MTS assay for cell proliferation after 0, 24, 48, and 72 h transfection. **D**, and **E**, Western blot for Ki-67 and PCNA levels 48 h after transfection. **F**, and **G**, Western blot for the expression of LC3B-II, LC3B-I, and p62 after 48 h transfection in transfected cells. *$p<0.05$.

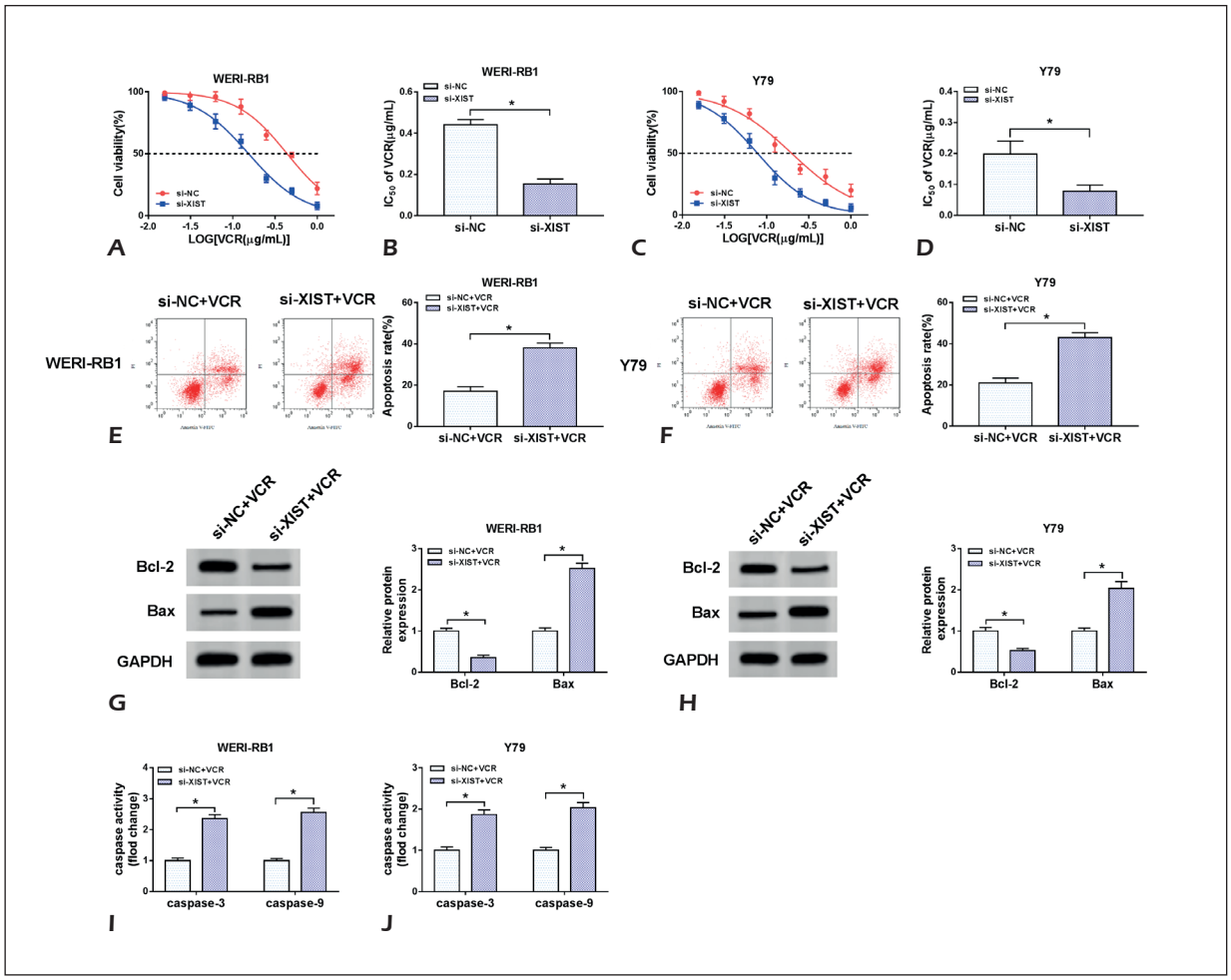

Figure 3. XIST silencing sensitized RB cell to VCR. **A-D**, WERI-RB1 and Y79 cells were transfected with si-NC or si-XIST for 24 h and then exposed to various concentrations (0, 0.015625, 0.03125, 0.0625, 0.125, 0.25, 0.5 and 1 μg/mL) of VCR for 48 h, followed by the detection of cell viability and IC50 value. WERI-RB1 and Y79 cells were transfected with si-NC or si-XIST for 24 h and then exposed to 0.1 μg/mL of VCR for 48 h, followed by the measurement of cell apoptosis by flow cytometry (**E** and **F**), the levels of Bcl-2 and Bax by Western blot (**G** and **H**), the activities of caspase-3 and caspase-9 using a corresponding assay kit (**I** and **J**). *p<0.05.

XIST Acted as a Molecular Sponge of MiR-204-5p

To further understand the underlying mechanism by which XIST regulated RB cell behaviors, we used online software starBase v.3 to help identify the directly interacted miRNAs of XIST. Among these candidates, miR-204-5p was of particular interest since it was discovered to play a tumor suppressive role in RB[18,19]. The predicted data revealed a putative complementary site for miR-204-5p in XIST (Figure 4A). To verify this, Luciferase reporter plasmids harboring the target sequence or mutated complementary sequence were transfected into WERI-RB1 and Y79 cells, respectively, together with miR-NC mimic or miR-204-5p mimic. With wild-type reporter and miR-204-5p overexpression caused a significant reduction in Luciferase activity (Figure 4B and 4C). However, the mutant-type reporter no longer elicited such an effect in the presence of miR-204-5p mimic (Figure 4B and 4C). These results indicated that XIST directly interacted with miR-204-5p through the complementary seed region. Additionally, the data of qRT-PCR showed a prominent downregulation of miR-204-5p in RB tissues and cells compared to their counterparts (Figure 4D and 4E). Also, an inverse correlation between XIST level and miR-204-5p expression was found in RB tissues (Figure 4F). Moreover, in contrast to a corresponding control, miR-204-5p expression was markedly elevated when XIST silencing, while it was strongly reduced by the transfection of pcDNA-XIST in the two RB cells (Figure 4G and 4H).

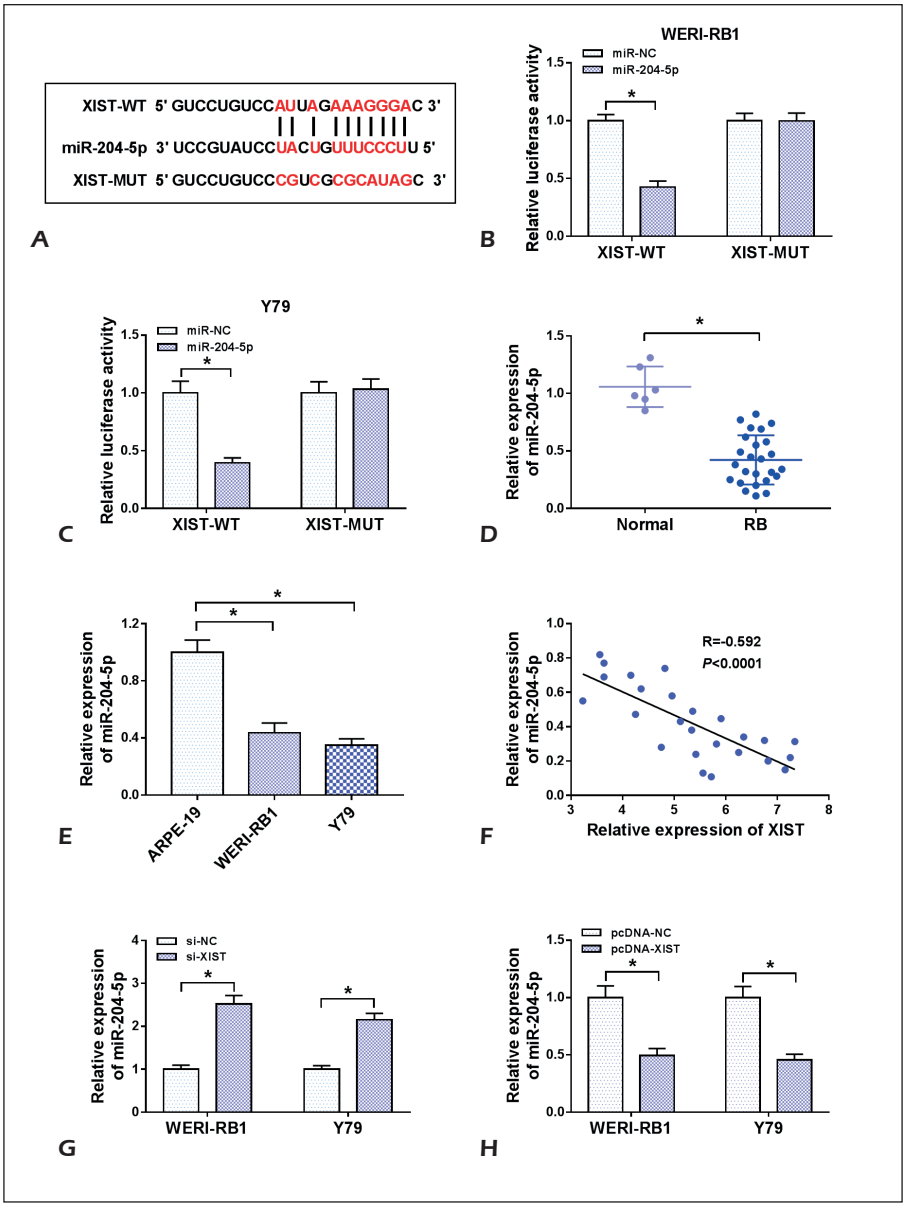

Figure 4. XIST acted as a miR-204-5p sponge. **A**, Schematic of the complementary sequence for miR-204-5p in XIST and mutated miR-204-5p-binding sequence. **B**, and **C**, Relative Luciferase activity in WERI-RB1 and Y79 cells cotransfected with XIST-WT or XIST-MUT and miR-NC mimic or miR-204-5p mimic. **D**, and **E**, The expression of miR-204-5p by qRT-PCR in RB tissues and the matched normal retinal tissues, ARPE-19, WERI-RB1, and Y79 cells. **F**, The correlation between XIST level and miR-204-5p expression in RB tissues using the Spearman test. **G**, and **H**, The expression of miR-204-5p in WERI-RB1 and Y79 cells transfected with si-NC, si-XIST, pcDNA-NC, or pcDNA-XIST. *$p<0.05$.

The Suppressive Effects of XIST Silencing on RB Cell Proliferation and Autophagy Were Reversed by Restored MiR-204-5p Expression

To provide further mechanistic insight into the link between XIST and miR-204-5p on RB cell behaviors, WERI-RB1 and Y79 cells were introduced with si-XIST and anti-miR-204-5p. As demonstrated by qRT-PCR, si-XIST-mediated miR-204-5p augmentation was significantly abolished by the co-transfection of anti-miR-204-5p in the two cells (Figure 5A and 5B). Subsequently, the analyses of MTS and Western blot revealed that compared to the negative group, the inhibition of XIST silencing on cell proliferation, Ki-67 and PCNA expression was highly reversed by restored miR-204-5p expression (Figure 5C-5F). Moreover, si-XIST-mediated anti-autophagy effect was remarkably abated by anti-miR-204-5p co-transfection in the two cells, as evidenced by the restoration of LC3B-II/I ratio and p62 expression (Figure 5G and 5H).

MiR-204-5p Mediated the Promotional Effect of XIST Silencing on RB Cell Sensitivity to VCR

In comparison to a corresponding negative control, the decreased IC_{50} value by XIST knockdown was prominently abolished by the restored miR-204-5p expression in both WERI-RB1 and

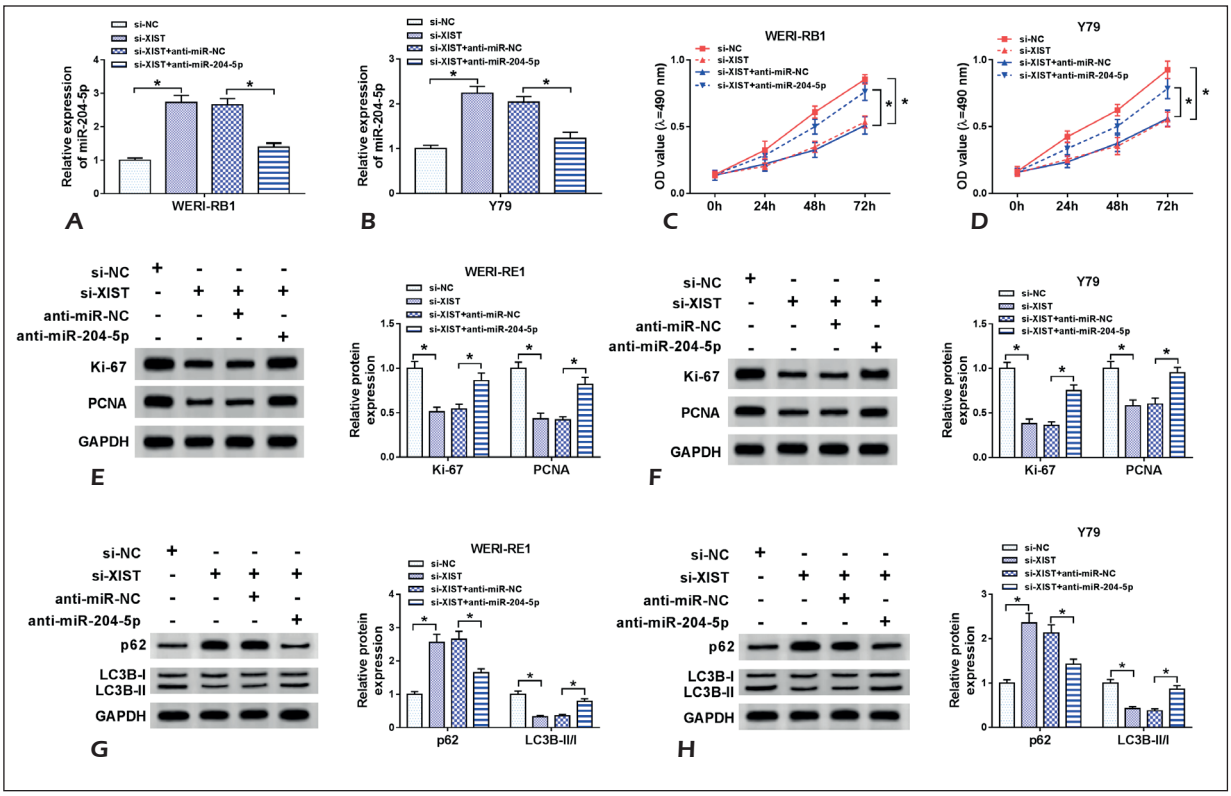

Figure 5. XIST silencing repressed RB cell proliferation and autophagy by up-regulating miR-204-5p. qRT-PCR for miR-204-5p expression (**A** and **B**), MTS assay for cell proliferation (**C**, and **D**,), Western blot for Ki-67 and PCNA levels (**E**,and **F**), Western blot for LC3B-II, LC3B-I and p62 levels (**G** and **H**) in WERI-RB1 and Y79 cells transfected with si-NC, si-XIST, si-XIST+anti-miR-NC or si-XIST+anti-miR-204-5p. *p<0.05.

Y79 cells (Figure 6A-6D). Moreover, the regulatory effects of XIST silencing on cell apoptosis (Figure 6E and 6F), Bcl-2 and Bax levels (Figure 6G and 6H), as well as caspase-3 and caspase-9 activities (Figure 6I and 6J) after VCR treatment were significantly reversed by the restored expression of miR-204-5p in the two RB cells.

Silencing of XIST Retarded Tumor Growth and Promoted VCR Sensitivity In Vivo

We further explored the impact of XIST on tumor growth and VCR sensitivity *in vivo* using xenograft model. These results revealed that compared with their counterparts, VCR treatment or sh-XIST transduction significantly hindered tumor growth, as presented by the reduction of tumor volume (Figure 7A) and weight (Figure 7B). Moreover, simultaneous VCR treatment and sh-XIST transduction resulted in a more significant repression on tumor growth (Figure 7A and 7B), suggesting that sh-XIST transduction promoted VCR-induced anti-cancer function. Additionally, the data of qRT-PCR showed that XIST was down-regulated and miR-204-5p was up-regulated in tumor tissues derived from sh-XIST-transduced Y79 cells with or without VCR treatment (Figure 7C and 7D).

Discussion

LncRNAs are emerging classes of regulatory transcripts that play crucial roles in human cancers, including RB[7]. Among these candidates, XIST was particularly attractive in the present work considering the important involvement of XIST in cancer biology[22]. In the preliminary stage of this study, we predicted a putative complementary site between XIST and miR-204-5p using online software starBase v.3. The current work had led to the identification of XIST silencing that weakened the proliferation and autophagy and promoted VCR sensitivity of RB cells through upregulating miR-204-5p by direct interaction.

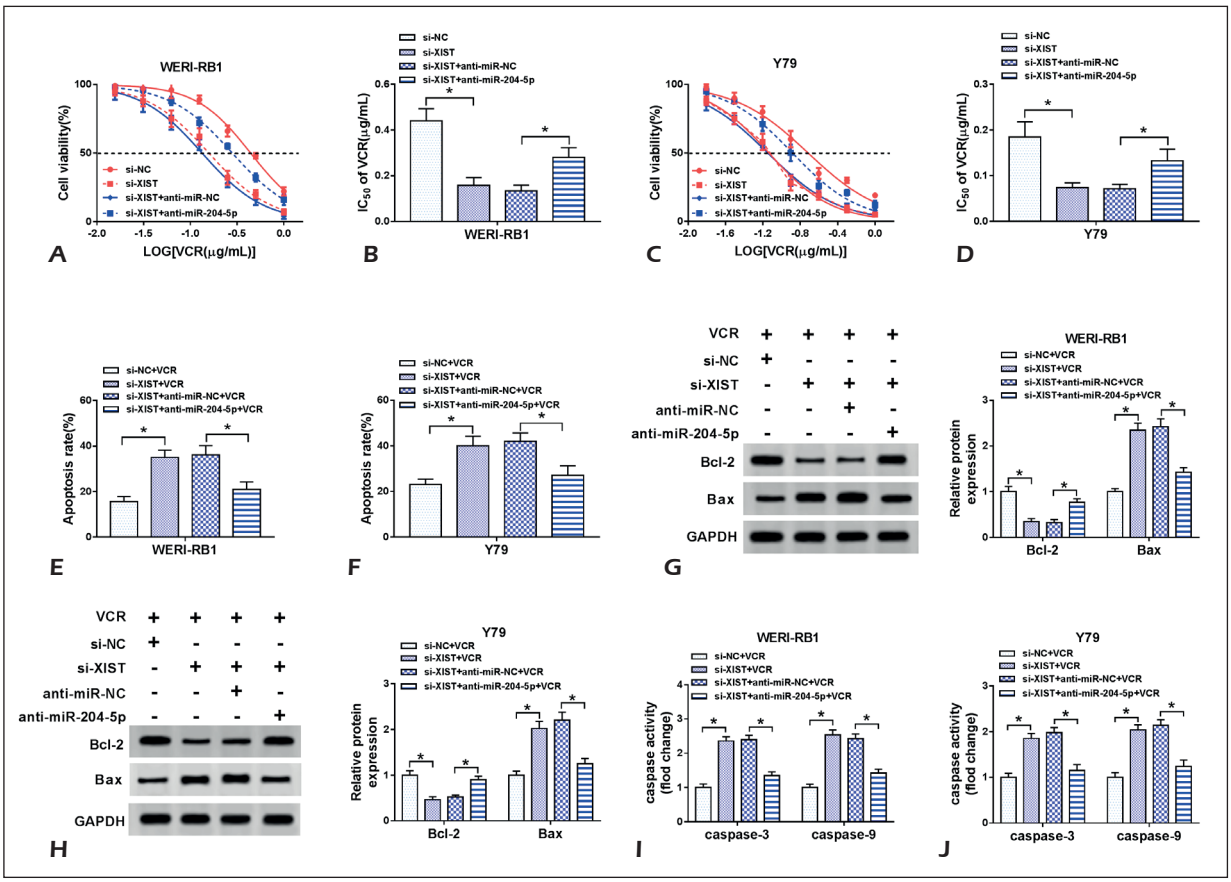

Figure 6. XIST silencing sensitized RB cells to VCR by the up-regulation of miR-204-5p. **A**-**D**, Determination of IC50 value in WERI-RB1 and Y79 cells transfected with si-NC, si-XIST, si-XIST+anti-miR-NC or si-XIST+anti-miR-204-5p before various concentrations of VCR treatment. WERI-RB1 and Y79 cells were transfected with si-NC, si-XIST, si-XIST+anti-miR-NC or si-XIST+anti-miR-204-5p before 0.1 μg/mL of VCR treatment, followed by the measurement of cell apoptosis by flow cytometry (**E** and **F**), the levels of Bcl-2 and Bax by Western blot (**G** and **H**), the activities of caspase-3 and caspase-9 using a corresponding assay kit (**I** and **J**). *p<0.05.

In the current work, firstly, we validated that XIST was up-regulated in RB tissues and cells, consistent with recent researches[16,17]. The LC3B-II/I ratio and p62 level are widely acknowledged to reflect the activity of autophagy[23]. Our data also demonstrated a higher of LC3B-II/I ratio and a lower p62 expression in RB tissues compared with the matched normal control, implying the activated cell autophagy in RB. Using loss-of-function experiments, our study confirmed that XIST silencing repressed proliferation, and promoted apoptosis of RB cells, in line with recent reports[16,17]. Moreover, we were first to uncover that XIST knockdown mitigated the autophagy of RB cells. Similar to our findings, Sun et al[15] reported that the depletion of XIST declined cell autophagy via regulating miR-17/autophagy-related gene 7 (ATG7) axis in non-small cell lung. Xie et al[24] demonstrated that a high level of XIST drove the autophagy of ethanol-induced hepatic stellate cells by sponging miR-29b and modulating high-mobility group box-1. Additionally, subcellular localization analysis revealed that XIST was prominently present in the cytoplasm. MiRNAs are known to be present in the cytoplasm in the form of the RNA-induced silencing complex[25]. These data provided evidence for the potential interplay between XIST and miRNAs in RB cells.

VCR has been generally accepted as a mainstay of treatment of many childhood cancers[26] and lncRNA expression is associated with VCR sensitivity in tumor cells[27]. Xia et al[28] manifested that lncRNA maternally expressed gene 3 (MEG3) enhanced lung cancer cell sensitivity to VCR through the inhibition of autophagy. Ding et al[29] underscored that lncRNA gastric cancer-associated transcript 1 (GACAT1) promoted gastric cancer cell VCR sensitivity by the phosphatase

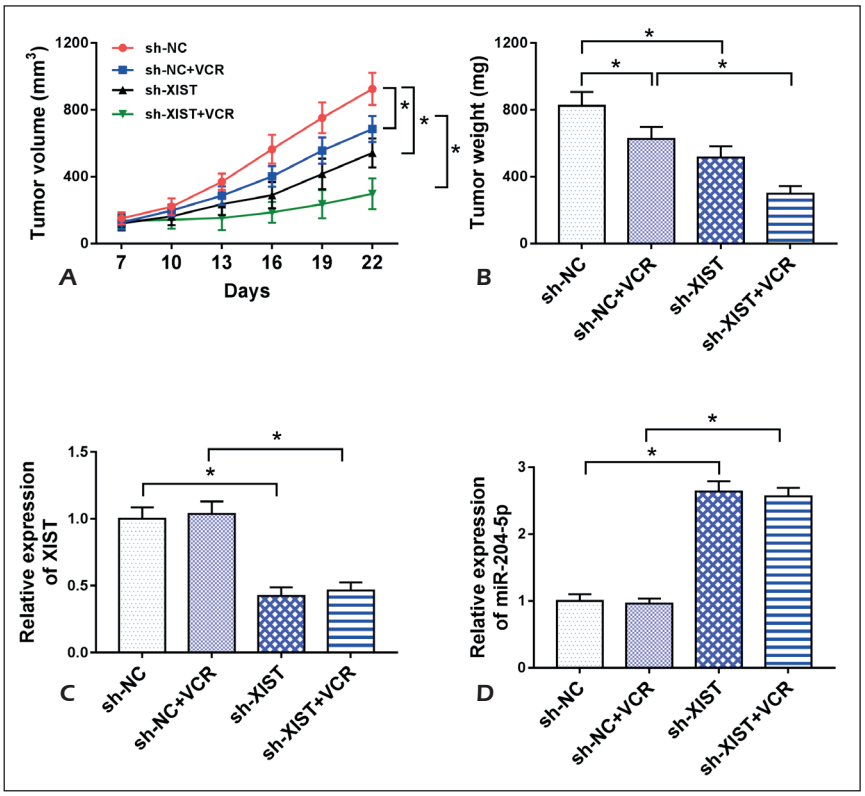

Figure 7. XIST silencing mitigated tumor growth and enhanced VCR sensitivity in vivo. Y79 cells stably transduced sh-NC or sh-XIST were subcutaneously inoculated into the nude mice, followed by the administration with VCR (1 mg/kg) every 3 days. Twenty-two days later, all mice were euthanized, and tumor tissues were excised. **A**, After 7 days implantation, tumor volume measurement began and was conducted every 3 days. **B**, Xenograft tissues were weighted, and the average weight was calculated. qRT-PCR for XIST (**C**) and miR-204-5p (**D**) expression in tumor tissues. *p<0.05.

and tensin homolog (PTEN)/AKT/mTOR signaling pathway. In the current research, we first showed that XIST depletion sensitized RB cell to VCR through regulating apoptosis. Besides, some researches have reported that lncRNA could suppress the apoptosis of tumor cells by regulating autophagy[30,31]. Therefore, we inferred that XIST knockdown might enhance RB cells apoptosis by repressing autophagy.

Then, we used starBase v.3 software to help identify the potential miRNAs binding to XIST. From these data, miR-204-5p was selected for further experiments due to its key involvement in many types of human cancers, including osteosarcoma, esophageal squamous cell carcinoma and prostate cancer[32-34]. Moreover, miR-204-5p augmented chemotherapeutic sensitivity of colorectal cancer and prostate cancer[34,35]. In this study, we were first to verify that XIST functioned as a miR-204-5p sponge. Our results also demonstrated a significant reduction of miR-204-5p level in RB tissues and cells, in accordance with earlier studies[18,19]. Furthermore, our data first substantiated that the suppression of XIST silencing on RB cell proliferation and autophagy and the promotion on VCR sensitivity were mediated by miR-204-5p. Zhong et al[36] showed that lncRNA nuclear paraspeckle assembly transcript 1 (NEAT1) acted as a ceRNA of miR-204-5p to enhance RB cell proliferation and migration and inhibit apoptosis through modulating C-X-C chemokine receptor type 4 (CXCR4). Therefore, more researches about the downstream genes of the novel regulatory network in RB autophagy and VCR sensitivity will be performed in further work.

Lastly, the xenograft model assays demonstrated that XIST silencing repressed tumor growth and promoted tumor cell sensitivity to VCR *in vivo*. Moreover, XIST depletion triggered a significant increase in miR-204-5p expression in xenograft tissues, eliciting that XIST silencing weakened tumor growth and enhanced VCR sensitivity possibly by upregulating miR-204-5p.

Conclusions

The current study suggested that XIST silencing hampered RB progression and promoted VCR sensitivity *in vitro* and *in vivo* partially by acting as a sponge of miR-204-5p. Our research provid-

ed novel evidence that XIST might be a tumor promoter in RB and targeting XIST might be a potent therapeutic strategy for RB treatment.

Availability of Data and Materials

The analyzed data sets generated during the present study are available from the corresponding author on reasonable request.

Ethics Approval and Consent to Participate

The present study was approved by the Ethical Review Committee of Tianjin Medical University General Hospital.

Conflict of Interests

The authors declare that they have no conflict of interests.

References

1) Rao R, Honavar SG. Retinoblastoma. Indian J Pediatr 2017; 84: 937-944.
2) Mendoza PR, Grossniklaus HE. The biology of retinoblastoma. Prog Mol Biol Transl Sci 2015; 134: 503-516.
3) Fabian ID, Onadim Z, Karaa E, Duncan C, Chowdhury T, Scheimberg I, Ohnuma SI, Reddy MA, Sagoo MS. The management of retinoblastoma. Oncogene 2018; 37: 1551-1560.
4) Anastasiadou E, Jacob LS, Slack FJ. Non-coding RNA networks in cancer. Nat Rev Cancer 2018; 18: 5-18.
5) Fatica A, Bozzoni I. Long non-coding RNAs: new players in cell differentiation and development. Nat Rev Genet 2014; 15: 7-21.
6) Oliveto S, Mancino M, Manfrini N, Biffo S. Role of microRNAs in translation regulation and cancer. World J Biol Chem 2017; 8: 45-56.
7) Yang M, Wei W. Long non-coding RNAs in retinoblastoma. Pathol Res Pract 2019; 215: 152435.
8) Liu S, Yan G, Zhang J, Yu L. Knockdown of long noncoding RNA (lncRNA) metastasis-associated lung adenocarcinoma transcript 1 (MALAT1) inhibits proliferation, migration, and invasion and promotes apoptosis by targeting miR-124 in retinoblastoma. Oncol Res 2018; 26: 581-591.
9) Yan G, Su Y, Ma Z, Yu L, Chen N. Long noncoding RNA LINC00202 promotes tumor progression by sponging miR-3619-5p in retinoblastoma. Cell Struct Funct 2019; 44: 51-60.
10) Wang JX, Yang Y, Li K. Long noncoding RNA DANCR aggravates retinoblastoma through miR-34c and miR-613 by targeting MMP-9. J Cell Physiol 2018; 233: 6986-6995.
11) Chen DL, Chen LZ, Lu YX, Zhang DS, Zeng ZL, Pan ZZ, Huang P, Wang FH, Li YH, Ju HQ, Xu RH. Long noncoding RNA XIST expedites metastasis and modulates epithelial-mesenchymal transition in colorectal cancer. Cell Death Dis 2017; 8: e3011.
12) Fang J, Sun CC, Gong C. Long noncoding RNA XIST acts as an oncogene in non-small cell lung cancer by epigenetically repressing KLF2 expression. Biochem Biophys Res Commun 2016; 478: 811- 817.
13) Lv GY, Miao J, Zhang XL. Long noncoding RNA XIST promotes osteosarcoma progression by targeting ras-related protein RAP2B via miR-320b. Oncol Res 2018; 26: 837-846.
14) Zhu J, Zhang R, Yang D, Li J, Yan X, Jin K, Li W, Liu X, Zhao J, Shang W, Yu T. Knockdown of long non-coding RNA XIST inhibited doxorubicin resistance in colorectal cancer by upregulation of miR-124 and downregulation of SGK1. Cell Physiol Biochem 2018; 51: 113-128.
15) Sun W, Zu Y, Fu X, Deng Y. Knockdown of lncRNA-XIST enhances the chemosensitivity of NSCLC cells via suppression of autophagy. Oncol Rep 2017; 38: 3347-3354.
16) Hu C, Liu S, Han M, Wang Y, Xu C. Knockdown of lncRNA XIST inhibits retinoblastoma progression by modulating the miR-124/STAT3 axis. Biomed Pharmacother 2018; 107: 547-554.
17) Cheng Y, Chang Q, Zheng B, Xu J, Li H, Wang R. LncRNA XIST promotes the epithelial to mesenchymal transition of retinoblastoma via sponging miR-101. Eur J Pharmacol 2019; 843: 210-216.
18) Wu X, Zeng Y, Wu S, Zhong J, Wang Y, Xu J. MiR-204, down-regulated in retinoblastoma, regulates proliferation and invasion of human retinoblastoma cells by targeting CyclinD2 and MMP-9. FEBS Lett 2015; 589: 645-650.
19) Ding J, Lu X. Expression of miR-204 in pediatric retinoblastoma and its effects on proliferation and apoptosis of cancer cells. Oncol Lett 2018; 16: 7152-7157.
20) Hajirezaei M, Darbouy M, Kazemi B. Cloning and expression of the functional human anti-vascular endothelial growth factor (VEGF) using the pcDNA3.1 vector and the human chronic myelogenous leukemia cell line K562. Protein J 2014; 33: 100-109.
21) Liu X, Zhang Z, Ruan J, Pan Y, Magupalli VG, Wu H, Lieberman J. Inflammasome-activated gasdermin D causes pyroptosis by forming membrane pores. Nature 2016; 535: 153-158.
22) Chan JJ, Tay Y. Noncoding RNA: RNA regulatory networks in cancer. Int J Mol Sci 2018; 19. pii: E1310.
23) Barth S, Glick D, Macleod KF. Autophagy: assays and artifacts. J Pathol 2010; 221: 117-124.
24) Xie ZY, Wang FF, Xiao ZH, Liu SF, Lai YL, Tang SL. Long noncoding RNA XIST enhances ethanol-induced hepatic stellate cells autophagy and activation via miR-29b/HMGB1 axis. IUBMB Life 2019; 71: 1962-1972.
25) Iwakawa HO, Tomari Y. The functions of microRNAs: mRNA decay and translational repression. Trends Cell Biol 2015; 25: 651-665.

26) Moore AS, Norris R, Price G, Nguyen T, Ni M, George R, van Breda K, Duley J, Charles B, Pinkerton R. Vincristine pharmacodynamics and pharmacogenetics in children with cancer: a limited-sampling, population modelling approach. J Paediatr Child Health 2011; 47: 875-882.

27) Sun QL, Zhao CP, Wang TY, Hao XB, Wang XY, Zhang X, Li YC. Expression profile analysis of long non-coding RNA associated with vincristine resistance in colon cancer cells by next-generation sequencing. Gene 2015; 572: 79-86.

28) Xia H, Qu XL, Liu LY, Qian DH, Jing HY. LncRNA MEG3 promotes the sensitivity of vincristine by inhibiting autophagy in lung cancer chemotherapy. Eur Rev Med Pharmacol Sci 2018; 22: 1020-1027.

29) Ding H, Sun J, Li R, Wang G. Long non-coding RNA GACAT1 alleviates doxorubicin and vincristine resistance through a PTEN/AKT/mTOR/S6K1 regulatory pathway in gastric cancer. RSC Adv 2019; 9: 8048-8055.

30) Gao D, Lv AE, Li HP, Han DH, Zhang YP. LncRNA MALAT-1 elevates HMGB1 to promote autophagy resulting in inhibition of tumor cell apoptosis in multiple myeloma. J Cell Biochem 2017; 118: 3341-3348.

31) Yang Y, Chen D, Liu H, Yang K. Increased expression of lncRNA CASC9 promotes tumor progression by suppressing autophagy-mediated cell apoptosis via the AKT/mTOR pathway in oral squamous cell carcinoma. Cell Death Dis 2019; 10: 41.

32) Li M, Shen Y, Wang Q, Zhou X. MiR-204-5p promotes apoptosis and inhibits migration of osteosarcoma via targeting EBF2. Biochimie 2019; 158: 224-232.

33) Tang J, Li Z, Zhu Q, Wen W, Wang J, Xu J, Wu W, Zhu Y, Xu H, Chen L. MiR-204-5p regulates cell proliferation, invasion, and apoptosis by targeting IL-11 in esophageal squamous cell carcinoma. J Cell Physiol 2020; 235: 3043-3055.

34) Jiang X, Guo S, Zhang Y, Zhao Y, Li X, Jia Y, Xu Y, Ma B. LncRNA NEAT1 promotes docetaxel resistance in prostate cancer by regulating ACSL4 via sponging miR-34a-5p and miR-204-5p. Cell Signal 2020; 65: 109422.

35) Yin Y, Zhang B, Wang W, Fei B, Quan C, Zhang J, Song M, Bian Z, Wang Q, Ni S, Hu Y, Mao Y, Zhou L, Wang Y, Yu J, Du X, Hua D, Huang Z. MiR-204-5p inhibits proliferation and invasion and enhances chemotherapeutic sensitivity of colorectal cancer cells by downregulating RAB22A. Clin Cancer Res 2014; 20: 6187-6199.

36) Zhong W, Yang J, Li M, Li L, Li A. Long noncoding RNA NEAT1 promotes the growth of human retinoblastoma cells via regulation of miR-204/CXCR4 axis. J Cell Physiol 2019; 234: 11567-11576.